

Suppressing arrhythmias in cardiac models using overdrive pacing and calcium channel blockers

A. T. Stamp

*Center for BioDynamics and Department of Biomedical Engineering, Boston University,
44 Cummington Street, Boston, Massachusetts 02215*

G. V. Osipov

*Center for BioDynamics and Department of Biomedical Engineering, Boston University,
44 Cummington Street, Boston, Massachusetts 02215
and Department of Radiophysics, Nizhny Novgorod University, 23, Gagarin Avenue,
Nizhny Novgorod, 603600 Russia*

J. J. Collins^{a)}

*Center for BioDynamics and Department of Biomedical Engineering, Boston University,
44 Cummington Street, Boston, Massachusetts 02215*

(Received 7 February 2002; accepted 25 June 2002; published 23 August 2002)

Recent findings indicate that ventricular fibrillation might arise from spiral wave chaos. Our objective in this computational study was to investigate wave interactions in excitable media and to explore the feasibility of using overdrive pacing to suppress spiral wave chaos. This work is based on the finding that in excitable media, propagating waves with the highest excitation frequency eventually overtake all other waves. We analyzed the effects of low-amplitude, high-frequency pacing in one-dimensional and two-dimensional networks of coupled, excitable cells governed by the Luo–Rudy model. In the one-dimensional cardiac model, we found narrow high-frequency regions of 1:1 synchronization between the input stimulus and the system's response. The frequencies in this region were higher than the intrinsic spiral wave frequency of cardiac tissue. When we paced the two-dimensional cardiac model with frequencies from this region, we found that spiral wave chaos could, in some cases, be suppressed. When we coupled the overdrive pacing with calcium channel blockers, we found that spiral wave chaos could be suppressed in all cases. These findings suggest that low-amplitude, high-frequency overdrive pacing, in combination with calcium channel inhibitors (e.g., class II or class IV antiarrhythmic drugs), may be useful for eliminating fibrillation. © 2002 American Institute of Physics. [DOI: 10.1063/1.1500495]

There is only one clinical method of treating a heart in ventricular fibrillation—applying a large voltage shock to the heart. Although the shock is of sufficient energy to annihilate fibrillation, it is also of sufficient strength to damage the underlying cardiac tissue, cause pain to the patient, and drain the battery of an implanted defibrillator. In this paper, we propose low-energy alternatives for defibrillation. We present computational findings which indicate that it may be possible to defibrillate cardiac tissue using low-amplitude, high-frequency pacing. We systematically explore the parameter space governing the pacing stimulus and present a map of the most promising stimulus waveforms. In addition, we show that the pacing technique can be optimized if it is used in conjunction with antiarrhythmic drugs, specifically those which block calcium channels. This novel defibrillation technique could be realized in a clinical setting by implanting both a drug pump and a pacemaker, and programming them so that they are simultaneously activated at the onset of fibrillation. Alternatively, long-term, low-dose oral calcium channel blockers could be administered in conjunction with an implanted pacemaker.

I. INTRODUCTION

Under sinus rhythm, waves of electrical activity propagate throughout the heart, eliciting a simultaneous contraction of the ventricles. However, in diseased heart tissue, tachycardias can develop when excitatory spiral waves locally re-excite tissue prior to the next stimulus from the sinoatrial node. Ventricular fibrillation might arise if these spiral waves break up into spiral wave chaos.^{1–4}

Current ventricular defibrillation techniques rely on the application of a large voltage shock to the heart. It is thought that this shock halts all electrical activity within the heart and prevents a local re-excitation of the tissue. Once the heart cells repolarize in synchrony, electrical waves from the sinoatrial node take over and a sinus rhythm resumes. However, the energy necessary for successful defibrillation using this technique is quite painful and often large enough to damage the tissue.⁵

A number of past experiments have explored the use of low-amplitude, high-frequency pacing (i.e., overdrive pacing) as an alternative defibrillation technique.^{6–11} In each experiment, the pacing had local effects, resulting in only small areas of organized electrical activity. Once the pacing was suspended, the local region of capture was re-invaded by surrounding electrical activity, and the tissue remained in a state of fibrillation. Thus, in all cases, overdrive pacing was

^{a)} Author to whom correspondence should be addressed. Telephone 617-353-0390; fax: 617-353-5462; electronic mail: jcollins@bu.edu

only marginally effective in eliminating the arrhythmia. It is important to note that the stimulation parameters, including stimulus waveform and input frequency, for each of these studies were similar. Specifically, each of these experiments utilized stimuli consisting of either monophasic square-wave pulses of 2 ms duration or symmetric biphasic square-wave pulses of 2 ms duration [see Figs. 5(A) and 5(B) of the present paper for example waveforms], and a pacing frequency slightly higher or lower than the average excitation frequency of the fibrillating tissue.

Extensive research has been done on the periodic pacing of spiral waves in excitable media.^{12–15} These studies have shown that a periodic train of pulses can eliminate spiral waves in an excitable medium if the frequency of the pacing wave is greater than that of the spiral wave. In effect, the high-frequency wave pushes the low-frequency wave beyond the edges of the medium, thereby suppressing its wavefronts. Sparse spiral waves can also be annihilated using a lower frequency pacing wave when the pacing source is close to the core of the spiral wave.¹⁶ It is important to note that each of these studies primarily explored the effects of the frequency of the periodic pacing on the spiral waves.

In this paper, we explore the feasibility of using overdrive pacing to eliminate spiral waves and spiral wave chaos in cardiac tissue. We base our *in numero* experiments on theoretical principles underlying the physics of interacting waves in excitable media, and we explore a stimulation parameter space that is considerably larger than that utilized in the aforementioned experimental and theoretical studies. In addition, we examine the possibility of coupling overdrive pacing with calcium channel blockers. Although calcium channel antagonists are often considered to be proarrhythmic,^{17,18} they also have been shown to transform spiral wave chaos into quasiperiodic, meandering spiral wave activity.¹⁸ We explore, in a series of computational experiments, the possibility of exploiting this effect to enhance the effectiveness of overdrive pacing in eliminating arrhythmias.

II. METHODS

A. Cardiac model

We conducted all of our computational experiments with a monophasic description of ventricular myocardium. The model is given by the expression,

$$C_m \frac{\partial V}{\partial t} = -I_{\text{ion}} - I_{\text{stimulus}} + C_m D \nabla^2 V,$$

where V is the membrane voltage, $C_m = 1 \mu\text{F}/\text{cm}^2$ is the membrane capacitance, $D = 0.001 \text{ cm}^2/\text{ms}$ is the diffusion coefficient, I_{stimulus} is the input stimulus, and I_{ion} is the sum of six ionic currents,

$$I_{\text{ion}} = I_{\text{Na}} + I_{\text{si}} + I_{\text{K}} + I_{\text{K1}} + I_{\text{Kp}} + I_b$$

as specified in the Luo–Rudy phase I model.¹⁹ The form of the sodium current I_{Na} , the slow inward calcium current I_{si} , and the potassium current I_{K} is given by

$$I_i = \bar{G}_i g_i(V, t)(V - E_i),$$

TABLE I. The conductance \bar{G}_i (mS/cm²) and reversal potential E_i (mV) for each current in the Luo–Rudy model. The reversal potential of I_{si} depends upon the internal calcium concentration, which varies with time.

i	\bar{G}_i (mS/cm ²)	E_i (mV)
Na	23	54.44
si	0.07	$7.7 - 13.0287 \cdot \ln([\text{Ca}]_i)$
K	0.705	-77
K1	0.6047	-87.23
Kp	0.0183	-87.23
b	0.03921	-59.87

where \bar{G}_i is the maximum constant conductance of the ion, $g_i(V, t)$ is the product of one or more gating variables, and E_i is the reversal potential of the ion. The dynamics of each gating variable is modeled as

$$\frac{dg_i}{dt} = \frac{g_\infty - g_i}{\tau_{gi}},$$

where $g_\infty = \alpha_{gi}/[\alpha_{gi} + \beta_{gi}]$ is the steady-state value, $\tau_{gi} = 1/[\alpha_{gi} + \beta_{gi}]$ is the time constant, and the α 's and β 's are functions of the membrane voltage. The form of the time-independent potassium current I_{K1} , the plateau potassium current I_{Kp} , and the background current I_b , is given by

$$I_i = \bar{A}_i(V - E_i),$$

where E_i is the reversal potential of the ion and \bar{A}_i is a scaling factor. Note that \bar{A}_i is a function of voltage for I_{K1} and I_{Kp} . The conductances and reversal potentials used in the simulations are listed in Table I.

B. Theoretical basis of our approach

The behavior of interacting waves in homogeneous excitable media is governed by the following fundamental properties:

- (1) *The wave with the highest frequency will eventually overtake all other waves.*^{12,15,20} This is due to the fact that slower waves are progressively invaded by faster waves.
- (2) *A given medium typically supports interacting spiral waves of a single frequency.*^{12,21} When spiral waves of different frequencies are interacting in a single medium, the wave with the highest frequency will dominate according to the first property. Thus, only waves of a single frequency can eventually coexist in a given medium. This characteristic arises from general properties of the system's action potential, in particular, its refractory period. The spiral wave frequency varies from medium to medium, even though a unique frequency exists for every medium. In human cardiac tissue, the intrinsic spiral wave frequency is approximately 6.3 Hz.²²
- (3) *Planar wavefronts travel faster than convex wavefronts.*²³ In traveling waves with significant positive curvature, every successive time step requires more cells to be excited. The additional transverse current load needed to support this expanding wavefront causes the curved wave to travel slower than a planar wave.

- (4) *The time to suppression of colliding periodic waves depends inversely on two factors: (i) the frequency difference between the waves, and (ii) the velocity of the wave with the highest frequency.*^{20,24} Thus, a slower wave is more quickly invaded by a faster wave as the frequency and/or velocity of the faster wave increases.

We used the above properties to guide our *in numero* experiments. For example, on the basis of the first and second properties, we explored pacing frequencies greater than the intrinsic spiral wave frequency of cardiac tissue. In addition, on the basis of the third property, we generated planar wavefronts by incorporating into the model the equivalent of a strip electrode. Finally, on the basis of the fourth property, we utilized the highest frequencies which could be produced in the medium.

In order to find the highest frequencies supported by the medium, we characterized the frequency response of the system by examining the synchronization between the applied stimulation and the resulting action potentials of the medium. Note that high-frequency stimuli in excitable media typically do not result in 1:1 synchronization between the input (pulse stimulus) and the response (action potential). This effect is due to the system's refractory period. At times, the cells in the medium may respond to every other pulse or every third pulse depending upon the refractory state, resulting in 2:1 or 3:1 synchronization; more complicated dynamics are also possible.^{25,26}

C. Computer simulations

We conducted computer simulations in one dimension using a chain of 30 cells, and in two dimensions using a network of 300×300 cells. The one-dimensional simulations were conducted to investigate the frequency response of the cardiac model to various stimuli. We then used the high-frequency regions of 1:1 synchronization found in the one-dimensional studies as the basis for exploring the elimination of spiral waves and spiral wave chaos in two dimensions.

The one-dimensional simulations were performed by stimulating the first cell in the 30-cell chain for 5.0 s and by averaging the action potential frequency of the last cell in the chain over the final 1.0 s of the computational trial. In the one-dimensional case, the output frequency (i.e., the action potential frequency of the last cell) is well-defined because the excitatory stimulus propagates in only one direction. However, in the two-dimensional case, the output frequency is not as clearly defined because excitatory stimuli can flow into a cell from four directions, often causing action potentials to be produced before the cell returns to its resting potential. In our simulations, we neglected changes in action potential morphology over time, and we grouped all K:K synchronization regions, where K is a positive integer, into the 1:1 synchronization region. We similarly grouped all 2K:K synchronization regions into the 2:1 synchronization region.

We used two integration methods for the simulations: the forward Euler (FE) method and the operator splitting (OS) method.^{27,28} The FE approach was implemented with a fixed time step of 0.01 ms, and the OS method was implemented

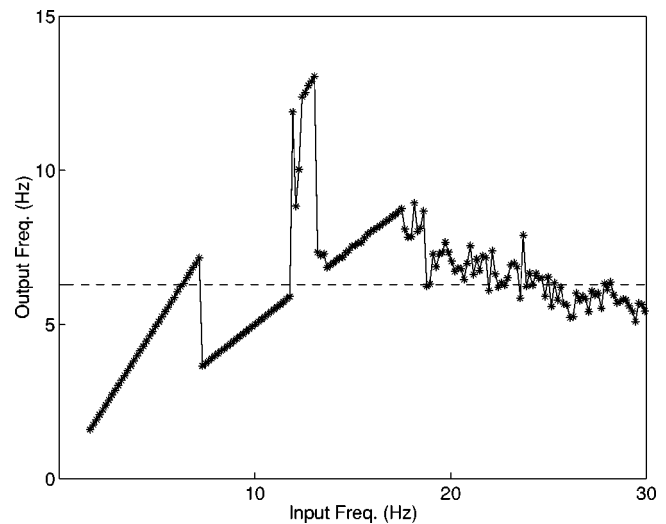


FIG. 1. Output frequency versus input frequency for a driven one-dimensional chain of 30 cells. The stimulus consisted of a square wave with an amplitude of 100 $\mu\text{Amp}/\text{cm}^2$ and a duty cycle of 50%. The dashed horizontal line at 6.3 Hz represents the spiral wave frequency of cardiac tissue.

with an adaptive time step ranging from 0.05 to 0.005 ms. We simulated isotropic media with a spatial step of 0.028 cm, and we used the following no-flux boundary conditions for all simulations:

$$\left. \frac{\partial V}{\partial x} \right|_{x=0} = \left. \frac{\partial V}{\partial x} \right|_{x=L} = \left. \frac{\partial V}{\partial y} \right|_{y=0} = \left. \frac{\partial V}{\partial y} \right|_{y=L} = 0,$$

where L is the tissue length.

III. RESULTS

A. One-dimensional simulations

In our first series of computational experiments, we periodically paced the one-dimensional chain of 30 cells with a square-wave stimulus (amplitude = 100 $\mu\text{Amp}/\text{cm}^2$). The input-output frequency characterization for this system is shown in Fig. 1. The spiral wave frequency for cardiac tissue is shown as a horizontal dashed line at 6.3 Hz. Thus, an output frequency greater than this line could potentially result in the suppression of spiral waves. The initial straight line represents 1:1 synchronization, or multiples thereof, in which the system responds to every input stimulus. Beginning at an input frequency of 7.3 Hz, the system responds to every other pulse resulting in 2:1 synchronization. Interestingly, the system returns to 1:1 synchronization, intermittent within the 2:1 synchronization region. This narrow 1:1 intermittency region centered around an input frequency of 12.7 Hz (Fig. 1) appears to be a promising region for suppression.

We explored the effects of pulse duration on the system's input-output frequency response by varying the percentage of cycle time (the duty cycle) that the square-wave pulse was greater than zero. The results for a range of duty cycles are shown in Fig. 2. It can be seen that for the duty cycles included in this figure, the 1:1 intermittency region only appears for the 50% value. Moreover, we found that the 2:1 synchronization region breaks up as the duty cycle decreases.

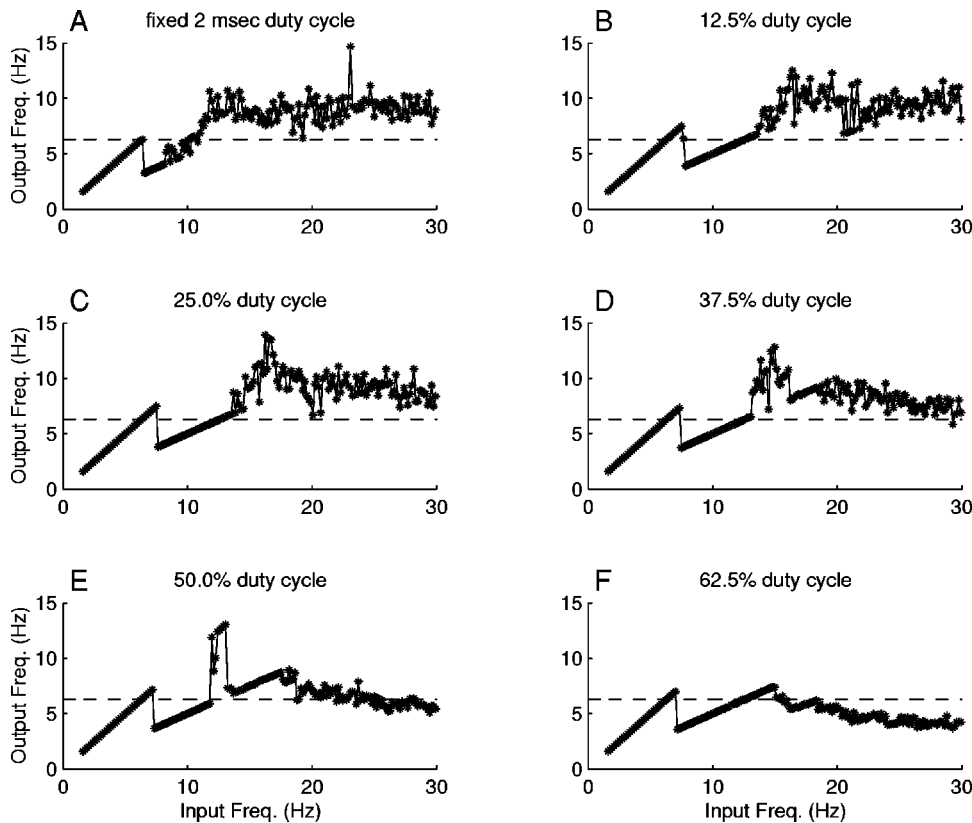


FIG. 2. Plots of output frequency versus input frequency for a driven one-dimensional chain of 30 cells. The stimulus consisted of a square wave with an amplitude of $100 \mu\text{Amp}/\text{cm}^2$ and a duty cycle of (A) a fixed, 2 ms duration; (B) 12.5%; (C) 25.0%; (D) 37.5%; (E) 50.0%; and (F) 62.5%. As in Fig. 1, the dashed horizontal lines represent the intrinsic spiral wave frequency of 6.3 Hz. Note that Fig. 1 has been included as Fig. 2(E) for reference.

We next examined the effects of stimulus amplitude on the 1:1 and 2:1 synchronization regions. The results for various amplitudes, as a function of input frequency, are shown in Fig. 3. The 1:1 intermittency region seen in Fig. 1, curves toward lower frequencies and breaks up for smaller stimulus amplitudes. It is important to point out that 2:1 synchronization regions with output frequencies > 6.3 Hz, and thus input frequencies > 12.6 Hz, could potentially be useful for suppressing spiral waves as well. Thus, portions of the 2:1 synchronization region to the right of the 1:1 intermittency region in Fig. 3 may be effective for eliminating spiral waves in two-dimensional media.

Given the promising results for a duty cycle of 50% (Fig. 2), we further investigated the effects of stimulus amplitude on the 1:1 and 2:1 synchronization regions for duty cycles ranging from 40% to 60%. Figure 4 indicates that as the duty cycle is decreased from 50% to 40%, the 1:1 intermittency region breaks up, while the 2:1 synchronization region remains stable. Figure 4 also shows that as the duty cycle is increased beyond 50%, the 1:1 intermittency region is invaded by the surrounding 2:1 synchronization regions. These findings indicate that the 1:1 intermittency region quickly disappears if the duty cycle departs from a value of 50%.

We also examined the effects of stimulus waveform on the 1:1 and 2:1 synchronization regions. Figure 5 presents the results for six different waveforms. It can be seen that monophasic square-wave pulses of 2 ms duration [Fig. 5(A)] rarely result in 1:1 synchronization (only four data points over the explored parameter space resulted in 1:1 synchronization). Similar results are obtained if the medium is paced

with symmetric biphasic square-wave pulses of 2 ms duration [Fig. 5(B)]. We also found that sinusoidal inputs [Fig. 5(C)] do not lead to 1:1 synchronization at high frequencies, whereas stimuli with ramp wavefronts and vertical wavebacks [Fig. 5(D)] do result in large regions of 1:1 synchronization, including a 1:1 intermittency region. For stimuli with vertical wavefronts and ramp wavebacks [Fig. 5(E)], the branch of the initial 1:1 synchronization region disappears and the 1:1 intermittency region becomes scattered. The 1:1 intermittency region disappears entirely when a triangle waveform with a ramp wavefront and waveback [Fig. 5(F)] is used to excite the system.

We also investigated the effects of calcium channel antagonists on our one-dimensional cardiac model. We eliminated transmembrane calcium fluxes by setting $\bar{G}_{si} = 0$ throughout each *in numero* experiment. The input-output frequency response results for various duty cycles are shown in Fig. 6. First, note that the elimination of slow inward calcium currents serves to increase the intrinsic spiral wave frequency from 6.3 Hz to 25.0 Hz. Second, it can be seen in Fig. 6 that the calcium channel antagonists eliminate the intermittency regions found in the original model. Figure 6 indicates that it may only be possible to eliminate spiral waves using the combined action of calcium channel blockers and overdrive pacing with a narrow band of input frequencies around 27 Hz at duty cycles $\leq 37.5\%$.

B. Two-dimensional simulations

We used predictions from the one-dimensional simulations to explore the suppression of spiral waves and spiral

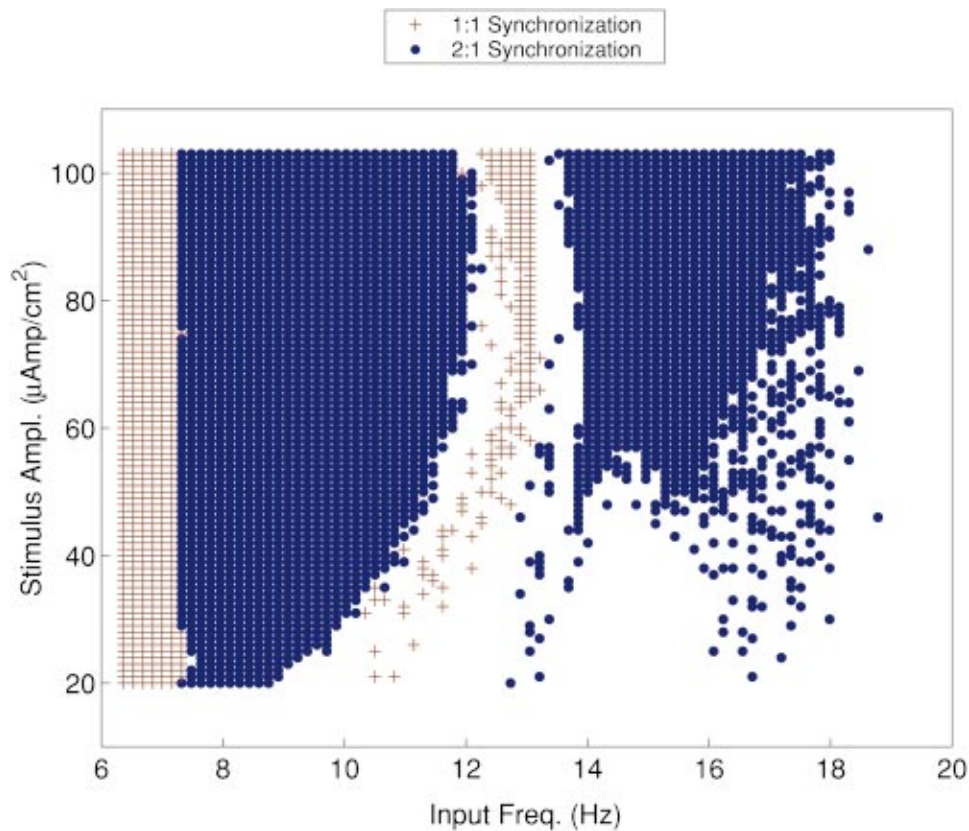


FIG. 3. (Color) Regions of 1:1 (red “+”) and 2:1 (blue “●”) synchronization, as a function of stimulus amplitude and input frequency, for a driven one-dimensional chain of 30 cells. The stimulus consisted of a square wave with a duty cycle of 50%.

wave chaos in two dimensions. For example, the results for the one-dimensional chain in Fig. 3 suggest that overdrive pacing the system at a frequency of 12.4 Hz with a square-wave stimulus of amplitude $50 \mu\text{Amp}/\text{cm}^2$ and duty cycle 50.0% should be sufficient for suppression. Figure 7 presents sequential snapshots of the two-dimensional cardiac model subject to such stimulation. Excitation was applied, starting at $t=0.00$ s, with a model equivalent of a strip electrode at the top of the medium to ensure a fast conduction velocity. Figure 7 shows that the initial spiral wave chaos ($t=0.00$ s) is entirely eliminated after 5.00 s of pacing. Pacing was continued beyond this point, and it can be seen that more-or-less planar wavefronts travel through the medium for at least one second (from $t=5.00$ s to $t=6.00$ s). Shortly thereafter, however, spiral wave chaos is reinitiated, as can be seen at $t=6.25$ s. Thus, there exists a window of opportunity, in this case of approximately 1.0 s, in which the medium is free of spiral wave chaos. If the pacing is halted during this window, the medium will be left in a resting state. These results show that controlled intervals of overdrive pacing can be used to suppress spiral wave chaos.

In general, however, we found limited success for suppressing spiral wave chaos in two-dimensional media using overdrive pacing alone. The high-frequency stimuli predicted from the one-dimensional studies did not always result in planar wavebacks during capture. In many cases, subsequent wavefronts approached the wavebacks of prior stimuli, encountering cells in various refractory states. This led, in

some instances, to the reinitiation of spiral wave chaos after local capture.

We next investigated the effects of coupling overdrive pacing with calcium channel blockers. The inward calcium current in our cardiac model serves to keep the membrane voltage elevated after the initial, sodium-dependent depolarization. By inhibiting this current, the absolute refractory period of each cell is effectively reduced. When a stimulus is then applied to the model, the waveform encounters fewer inexcitable cells and thus has a higher chance of entraining the spiral waves. As noted earlier, the reduced refractory period also leads to an increase in the intrinsic spiral wave frequency of the medium. We therefore had to increase the frequency of our overdrive pacing to keep the input frequency higher than that of the spiral wave activity within the medium.

We inhibited the calcium flux in the model by setting the maximum calcium conductance, \bar{G}_{si} , to zero after the first time-step in the simulations. Figure 8 presents the results of a computational experiment where the top two rows of cells were paced at a frequency of 27.9 Hz with a square-wave stimulus of amplitude $50 \mu\text{Amp}/\text{cm}^2$ and duty cycle 12.5%. Inhibiting the calcium flux causes the initial spiral wave chaos to conform to a more regular, quasiperiodic meander, which is consistent with previously reported results.²⁹ This dynamic effect allows the applied stimulation to entrain the medium progressively. After 4.0 s, the applied stimulation

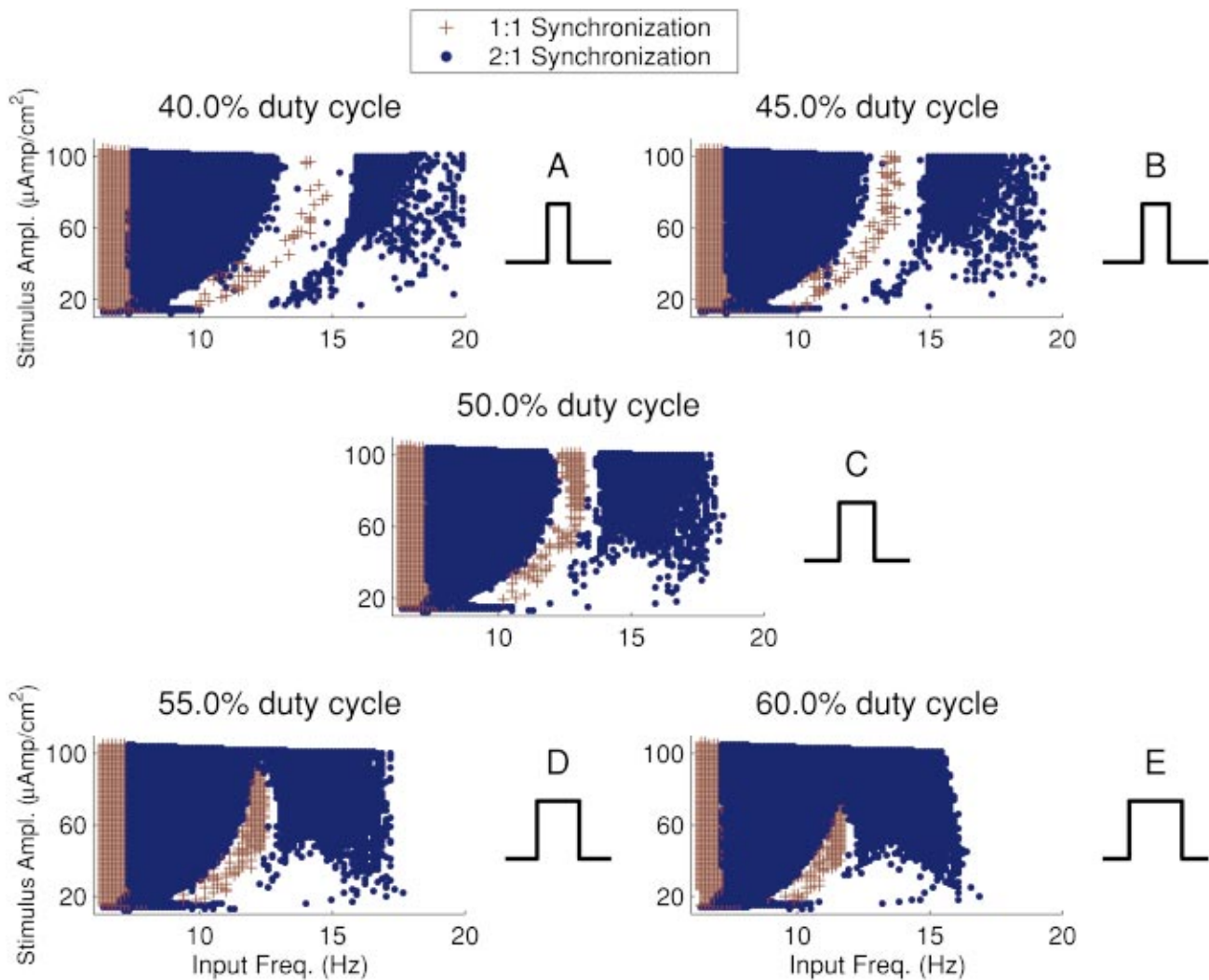


FIG. 4. (Color) Plots of 1:1 (red “+”) and 2:1 (blue “●”) synchronization regions, as a function of stimulus amplitude and input frequency, for a driven one-dimensional chain of 30 cells. The stimulus consisted of a square wave with a duty cycle of (A) 40%, (B) 45%, (C) 50%, (D) 55%, and (E) 60%. Note that Fig. 3 has been included as Fig. 4(C) for reference.

has annihilated all spiral wave activity within the medium (Fig. 8). When the stimulation is subsequently halted, the medium returns to its resting state within 270 ms.

We further explored the sensitivity of spiral wave suppression to the magnitude of the calcium current by repeating the above computational experiment with modified values of the maximum calcium conductance, \bar{G}_{si} . We found that spiral wave chaos could be suppressed similarly to that shown in Fig. 8 with reduced, nonzero levels of inward calcium current (\bar{G}_{si} greater than 0 but less than the nominal 0.07). However, the time to suppression of spiral wave chaos increased as the level of inward calcium current was increased. In general, we found more episodes of successful suppression of spiral wave chaos using the combined action of overdrive pacing and calcium channel antagonists, than in using overdrive pacing alone. In fact, we found that spiral wave chaos could be suppressed in all cases when the overdrive pacing was coupled with calcium channel blockers.

As it may not be possible to generate a completely planar wavefront outside of the computational realm, we also investigated the effects of using a point source to generate

convex waves in the cardiac model (data not shown). The experimental conditions were similar to those in Fig. 8, with the exception of the electrode geometry. We found that spiral wave chaos could be suppressed with a point source electrode; however, the time to suppression was longer than that for overdrive pacing with a strip electrode.

IV. DISCUSSION

In this work, we characterized the frequency response of a one-dimensional cardiac model to provide a map of the promising regions for suppressing spiral waves and spiral wave chaos in two dimensions. We used this information to guide our two-dimensional simulations and showed that it is possible to use overdrive pacing to eliminate spiral waves and spiral wave chaos in two-dimensional media. We also demonstrated that calcium channel blockers could be used to enhance the effectiveness of overdrive pacing in eliminating arrhythmias. Below, we discuss the implications of these findings.

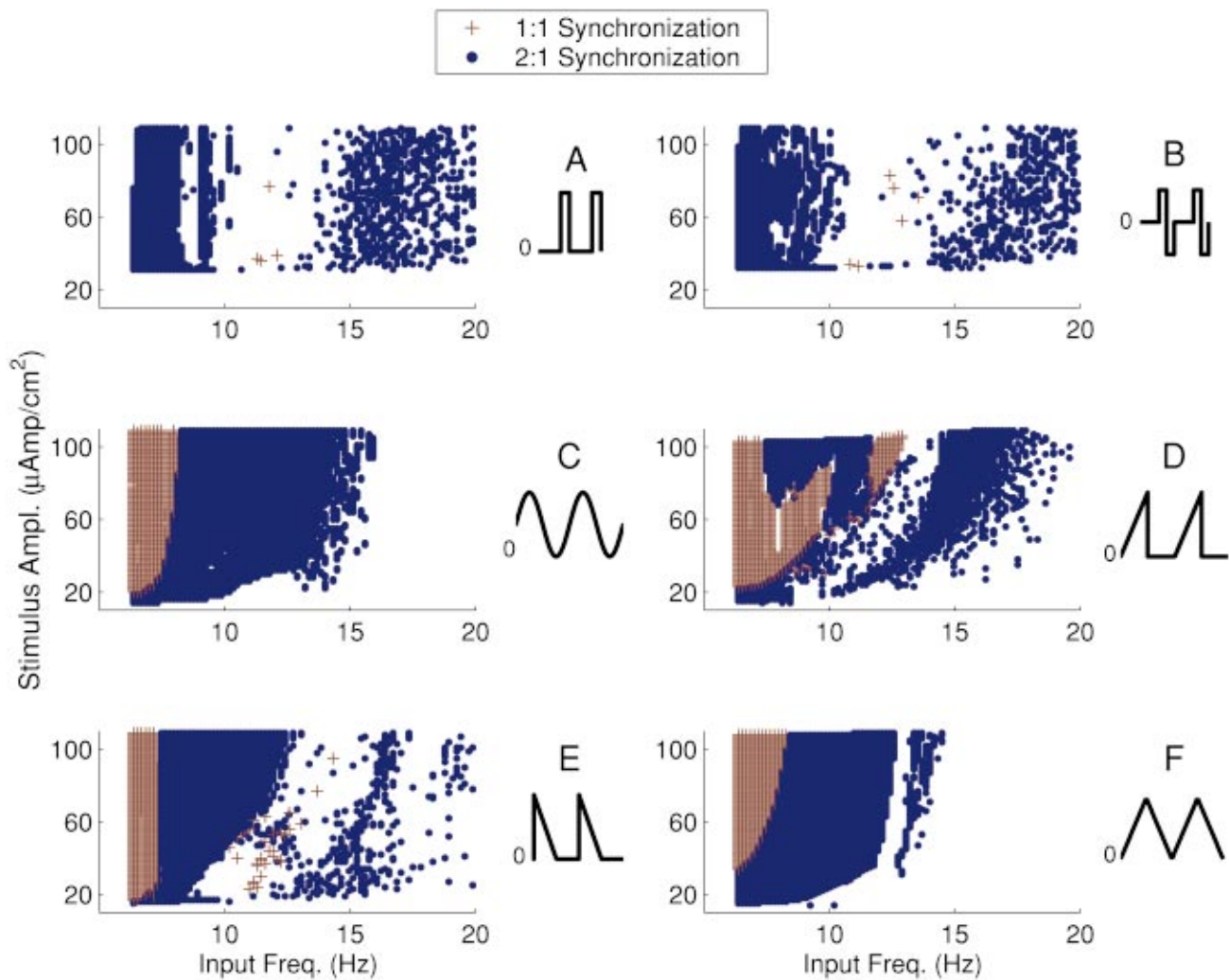


FIG. 5. (Color) Plots of 1:1 (red “+”) and 2:1 (blue “•”) synchronization regions, as a function of stimulus amplitude and input frequency, for a driven one-dimensional chain of 30 cells. The stimulus consisted of the following waveforms (shown to the right of each plot): (A) a monophasic square-wave pulse of 2 ms duration, (B) symmetric biphasic square-wave pulses of 2 ms duration, (C) a sine wave, (D) a waveform with a ramp wavefront and a vertical waveback, (E) a waveform with a vertical wavefront and a ramp waveback, and (F) a triangle wave.

A. In numero experiments

The results from our one-dimensional simulations can be used to guide the development of effective overdrive pacing schemes. For example, our findings indicate that the highest frequencies supported by the medium occur, in general, in the 1:1 intermittency region that arises for a duty cycle of 50%. We found that if the duty cycle is decreased, the intermittency region becomes irregular, resulting in lower output frequencies, and if the duty cycle is increased, the 1:1 intermittency region disappears. The presence of a high-frequency 1:1 intermittency region only at certain duty cycles (i.e., around 50%) may be due, in part, to the level of the applied current. At an appropriate duty cycle and current level, the input forces the system to respond to every pulse, even at high frequencies. At smaller duty cycles, the input may not be sufficiently strong to force the system to respond in a 1:1 fashion at high frequencies. Conversely, at larger duty cycles, the current level may be so high as to keep the cells depolarized, preventing sufficient time for recovery between pulses. In this case, the input would be unable to force the system to respond to every pulse.

The results of our one-dimensional simulations also show that high-frequency 1:1 intermittency regions arise only when certain waveforms are used. Specifically, we found that square waveforms (of sufficient duration) and waveforms with ramp wavefronts and vertical wavebacks give rise to robust, high-frequency 1:1 intermittency regions, whereas waveforms with vertical wavefronts and ramp wavebacks give rise to 1:1 intermittency regions at high frequencies that are scattered. In addition, we found that sinusoidal and triangle waveforms do not lead to any 1:1 synchronization at high frequencies. It is interesting to note that the two most effective waveforms, a square waveform and a waveform with a ramp wavefront and a vertical waveback, both possess a vertical waveback. It is possible that a vertical waveback enables cells to recover more quickly following an excitation, making them more responsive to high-frequency inputs. In contrast, a slowly decaying waveback, which injects current into a cell during its recovery, may prolong the refractory period by keeping the membrane voltage elevated. This would make a cell less responsive to high-frequency inputs.

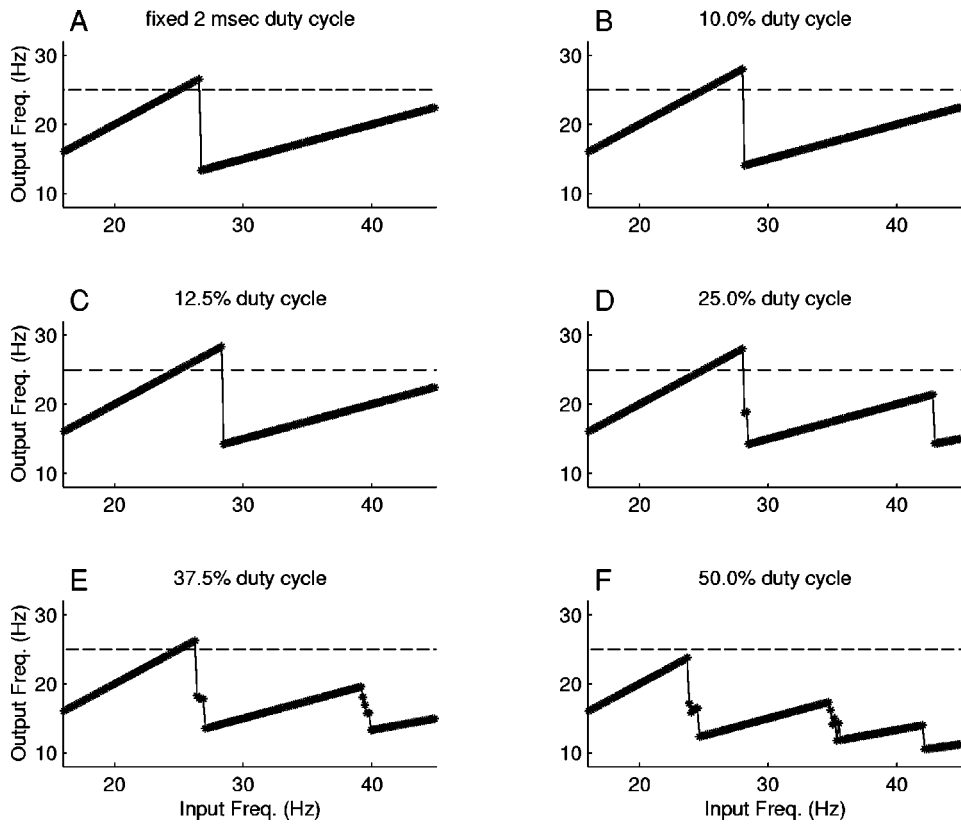


FIG. 6. Plots of output frequency versus input frequency for a driven one-dimensional chain of 30 cells. The calcium current was eliminated in the model by setting $\bar{G}_{si}=0$ throughout each *in numero* experiment. The stimulus consisted of a square wave with an amplitude of $100 \mu\text{Amp}/\text{cm}^2$ and a duty cycle of (A) a fixed, 2 ms duration; (B) 10.0%; (C) 12.5%; (D) 25.0%; (E) 37.5%; and (F) 50.0%. The dashed horizontal lines represent the intrinsic spiral wave frequency of 25.0 Hz.

We found that some, but not all, of the stimuli suggested by the one-dimensional simulations could be used to suppress spiral wave chaos in two-dimensional media. This discrepancy may be attributed to several factors. For instance, we found that the applied stimulation does not entrain the spiral wave chaos in a progressive manner. The nonprogressive suppression of spiral wave chaos as seen in Fig. 7 allows random excitation to re-excite tissue that had previously been entrained. This works against the intended suppression

and allows for a reinitiation of spiral wave chaos. In addition, the time to suppression in two dimensions may be longer than the duration of our simulations.

Our simulations also indicate that the elimination of slow inward calcium currents causes spiral wave chaos to conform to a more regular, quasiperiodic meandering spiral wave behavior, a pattern characteristic of ventricular tachycardia. We showed that if the cardiac model is additionally subjected to overdrive pacing, the meandering activity could

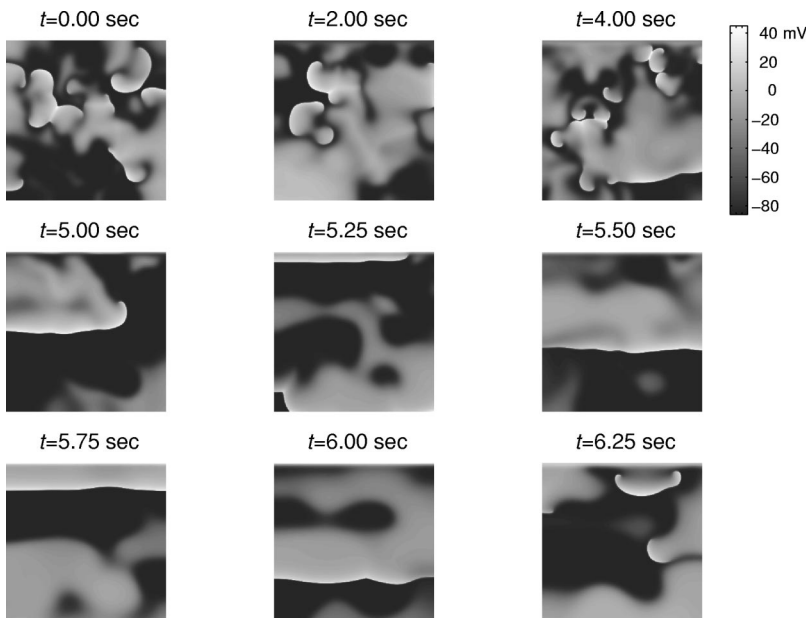


FIG. 7. Sequential time images of successful suppression of spiral wave chaos, using overdrive pacing, in a network of 300×300 cells. The system was excited with the model equivalent of a strip electrode of 2×300 cells located at the top border of the medium. The stimulus consisted of a square wave with an amplitude of $50 \mu\text{Amp}/\text{cm}^2$ and a duty cycle of 50.0%. The input frequency was 12.4 Hz. The membrane voltage (mV) of the cells in each image is color-coded as indicated in the bar located to the right of the top row of panels.

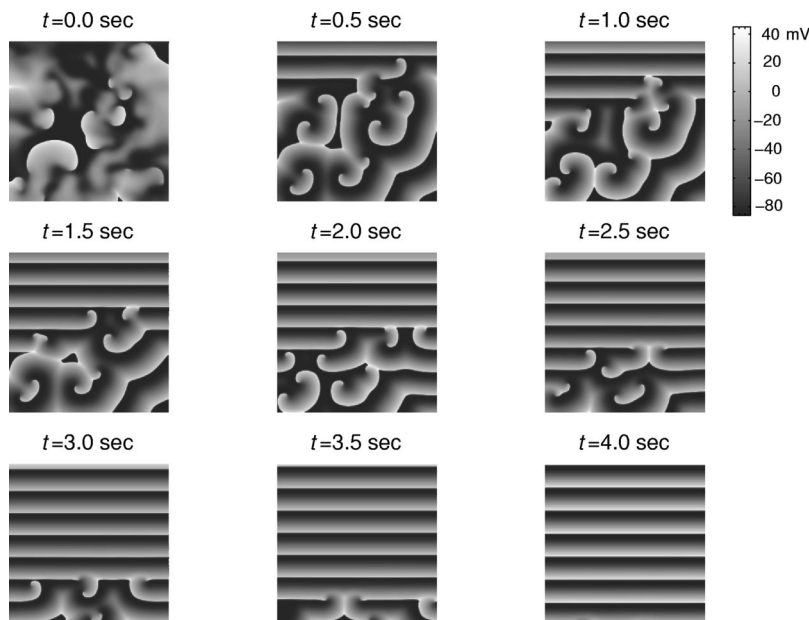


FIG. 8. Sequential time images of successful suppression of spiral wave chaos, using overdrive pacing in conjunction with calcium channel antagonists, in a network of 300×300 cells. The system was excited with the model equivalent of a strip electrode of 2×300 cells located at the top border of the medium. The stimulus consisted of a square wave with an amplitude of $50 \mu\text{A}/\text{cm}^2$ and a duty cycle of 12.5%. The input frequency was 27.9 Hz. The calcium channels in the model were blocked at $t=0.0$ s by setting $\bar{G}_{\text{si}}=0$. The membrane voltage (mV) of the cells in each image is color-coded as indicated in the bar located to the right of the top row of panels.

be suppressed. In a clinical setting, the calcium current can be inhibited by using class II or class IV antiarrhythmic drugs, which selectively block the inward calcium flux through the cell membrane. For example, Esmolol, a class II agent, and Verapamil, a class IV agent, could be delivered intravenously to inhibit the calcium flux selectively through the L-type calcium channel. Esmolol has a 1–2 min activation time with a half-life of 10 min, and Verapamil, in intravenous form, has an immediate onset of activation with a half-life of 4 min.^{30,31} These short-lived, fast-acting agents could be used to inactivate the calcium channels of the heart for short periods of time. Our simulations suggest that defibrillation could be attained if the drugs are delivered quickly in conjunction with overdrive pacing. In a clinical setting, this could be realized by implanting both a drug pump and a pacemaker, and programming them so that they are simultaneously activated at the onset of fibrillation. Alternatively, long-term, low-dose oral calcium channel blockers could be administered in conjunction with an implanted pacemaker.

B. Clinical significance

Our motivation for developing a technique for suppressing spiral waves and spiral wave chaos in excitable media stems from the potential of using such a technique for defibrillating cardiac tissue. The results of our simulations suggest that it may be possible to defibrillate cardiac tissue using low-amplitude, high-frequency pacing in the presence (or, more limitedly, in the absence) of calcium channel antagonists. By using the proper frequencies, amplitudes, and waveforms predicted from the one-dimensional simulations, we showed that it is possible to suppress spiral waves and spiral wave chaos in two-dimensional, excitable media. A clear next step is to confirm these results experimentally in animal models.

Experimental studies on the entrainment of ventricular fibrillation in porcine models¹¹ and atrial fibrillation in ca-

nine models^{6,10} and humans^{7–9} using rapid pacing have shown limited success, with the capture only of small, localized regions. However, the pacing frequencies used in these experiments were only slightly faster or slightly slower than the mean fibrillation frequency of the tissue. Our one-dimensional simulations suggest that frequencies approximately twice as high as the mean fibrillation frequency may be more appropriate for defibrillating cardiac tissue. It is also interesting to note that all of the aforementioned experimental studies utilized either monophasic square-wave pulses of 2 ms duration or symmetric biphasic square-wave pulses of 2 ms duration. However, Figs. 5(A) and 5(B) indicate that monophasic or biphasic square-wave pulses of 2 ms duration are not optimal if the goal is to obtain high-frequency responses from the system. Overall, our simulation results suggest that the aforementioned experiments^{6–11} should be expanded to include a broader range of frequencies and different stimulus waveforms, in addition to class II or class IV antiarrhythmic drugs.

ACKNOWLEDGMENTS

We thank Alan Garfinkel and Dave Christini for useful discussions. This work was supported by the U.S. National Science Foundation, the U.S. Department of Energy, and the Russian Fund for Basic Research (00-15-96582).

¹J. Jalife and R. A. Gray, "Drifting vortices of electrical waves underlie ventricular fibrillation in the rabbit heart," *Acta Physiol. Scand.* **157**, 123–131 (1996).

²J. Jalife, R. A. Gray, G. E. Morley, and J. M. Davidenko, "Self-organization and the dynamical nature of ventricular fibrillation," *Chaos* **8**, 79–93 (1998).

³A. V. Panfilov, "Spiral breakup as a model of ventricular fibrillation," *Chaos* **8**, 57–64 (1998).

⁴F. X. Witkowski, L. J. Leon, P. A. Penkoske, W. R. Giles, M. L. Spano, W. L. Ditto, and A. T. Winfree, "Spatiotemporal evolution of ventricular fibrillation," *Nature (London)* **392**, 78–82 (1998).

⁵L. Tung, "Detrimental effects of electrical fields on cardiac muscle," *Proc. IEEE* **84**, 366–378 (1996).

⁶M. Allesie, C. Kirchhof, G. J. Scheffer, F. Chorro, and J. Brugada, "Re-

- gional control of atrial fibrillation by rapid pacing in conscious dogs," *Circulation* **84**, 1689–1697 (1991).
- ⁷A. Capucci, F. Ravelli, G. Nollo, A. S. Montenero, M. Biffi, and G. Q. Villani, "Capture window in human atrial fibrillation," *J. Cardiovasc. Electrophysiol.* **10**, 319–327 (1999).
- ⁸E. G. Daoud, B. Pariseau, M. Niebauer, F. Bogun, R. Goyal, M. Harvey, K. C. Man, S. A. Strickberger, and F. Morady, "Response of type I atrial fibrillation to atrial pacing in humans," *Circulation* **94**, 1036–1040 (1996).
- ⁹J. M. Kalman, J. E. Olgin, M. R. Karch, and M. D. Lesh, "Regional entrainment of atrial fibrillation in man," *J. Cardiovasc. Electrophysiol.* **7**, 867–876 (1996).
- ¹⁰C. Kirchhof, F. Chorro, G. J. Scheffer, J. Brugada, K. Konings, Z. Zetelaki, and M. Allessie, "Regional entrainment of atrial fibrillation studied by high-resolution mapping in open-chest dogs," *Circulation* **88**, 736–749 (1993).
- ¹¹B. H. KenKnight, P. V. Bayly, R. J. Gerstle, D. L. Rollins, P. D. Wolf, W. M. Smith, and R. E. Ideker, "Regional capture of fibrillating ventricular myocardium: Evidence of an excitable gap," *Circ. Res.* **77**, 849–855 (1995).
- ¹²K. J. Lee, "Wave pattern selection in an excitable system," *Phys. Rev. Lett.* **79**, 2907–2910 (1997).
- ¹³R. Mantel and D. Barkley, "Periodic forcing of spiral waves in excitable media," *Phys. Rev. E* **54**, 4791–4802 (1996).
- ¹⁴A. T. Winfree, "Alternative stable rotors in an excitable medium," *Physica D* **49**, 125–140 (1991).
- ¹⁵F. Xie, Z. Qu, J. N. Weiss, and A. Garfinkel, "Interactions between stable spiral waves with different frequencies in cardiac tissue," *Phys. Rev. E* **59**, 2203–2205 (1999).
- ¹⁶G. Gottwald, A. Pumir, and V. Krinsky, "Spiral wave drift induced by stimulating wave trains," *Chaos* **11**, 487–494 (2001).
- ¹⁷A. L. Bassett, S. Chakko, and M. Epstein, "Are calcium antagonists proarrhythmic?" *J. Hypertens.* **15**, 915–923 (1997).
- ¹⁸T. R. Chay, "Why are some antiarrhythmic drugs proarrhythmic? Cardiac arrhythmia study by bifurcation analysis," *J. Electrocardiol.* **28**, 191–197 (1995).
- ¹⁹C. H. Luo and Y. Rudy, "A model of the ventricular cardiac action potential," *Circ. Res.* **68**, 1501–1526 (1991).
- ²⁰V. I. Krinsky and K. I. Agladze, "Interaction of rotating waves in an active chemical medium," *Physica D* **8**, 50–56 (1983).
- ²¹V. S. Zykov, "Spiral waves in two-dimensional excitable media," *Ann. N.Y. Acad. Sci.* **591**, 75–85 (1990).
- ²²A. T. Winfree, "Vortex action potentials in normal ventricular muscle," *Ann. N.Y. Acad. Sci.* **591**, 190–207 (1990).
- ²³J. J. Tyson and J. P. Keener, "Singular perturbation theory of traveling waves in excitable media," *Physica D* **32**, 327–361 (1988).
- ²⁴A. N. Zaikin and A. M. Zhabotinsky, "Concentration wave propagation in two-dimensional liquid-phase self-oscillating system," *Nature (London)* **225**, 535–537 (1970).
- ²⁵M. R. Guevara, A. Shrier, and L. Glass, "Phase-locked rhythms in periodically stimulated heart cell aggregates," *Am. J. Physiol.* **254**, H1–H10 (1988).
- ²⁶T. J. Lewis and M. R. Guevara, "Chaotic dynamics in an ionic model of the propagated cardiac action potential," *J. Theor. Biol.* **146**, 407–432 (1990).
- ²⁷Z. Qu and A. Garfinkel, "An advanced algorithm for solving partial differential equation in cardiac conduction," *IEEE Trans. Biomed. Eng.* **46**, 1166–1168 (1999).
- ²⁸S. Rush and H. Larsen, "A practical algorithm for solving dynamic membrane equations," *IEEE Trans. Biomed. Eng.* **25**, 389–392 (1978).
- ²⁹Z. Qu, J. N. Weiss, and A. Garfinkel, "From local to global spatiotemporal chaos in a cardiac tissue model," *Phys. Rev. E* **61**, 727–732 (2000).
- ³⁰P. O. Anderson, J. E. Knoben, and W. G. Troutman, *Handbook of Clinical Drug Data*, 9th ed. (Appleton and Lange, Stamford, 1999), pp. 345–357.
- ³¹S. C. Vlay, *A Practical Approach to Cardiac Arrhythmias*, 2nd ed. (Little, Brown, and Company, Boston, 1996), pp. 309–317.